

Effects of External and Internal Hyperthermia on LDL Transport and Accumulation Within an Arterial Wall in the Presence of a Stenosis

MARCELLO IASIELLO,^{1,2} KAMBIZ VAFAI,¹ ASSUNTA ANDREOZZI,² NICOLA BIANCO,² and FATEMEH TAVAKKOLI¹

¹Department of Mechanical Engineering, University of California, Riverside, CA 92521, USA; and ²Dipartimento di Ingegneria Industriale, Università degli Studi di Napoli Federico II, P.le Tecchio, 80, Naples 80125, Italy

(Received 1 October 2014; accepted 19 November 2014; published online 18 December 2014)

Associate Editor Estefanía Peña oversaw the review of this article.

Abstract—Effects of hyperthermia on transport of low-density lipoprotein (LDL) through a stenosed arterial wall are analyzed comprehensively in the present work. The realistic and pertinent aspects of an arterial wall is represented by a multi-layer model, with a proper representation of the thickened intima region due to the atherosclerotic plaque formation. Effects of external and internal hyperthermia on LDL concentration levels are established along with the range of influence of these effects. Various modules of the current work are comprehensively compared with pertinent literature and are found to be in excellent agreement. The effects of external and internal hyperthermia as well as the load level and the axial location of the plaque formation on LDL transport and accumulation for a stenosed artery are established in this work.

Keywords—LDL transport, Arterial wall, Hyperthermia, Accumulation.

NOMENCLATURE

A	Area reduction of the stenosis (m ²)
c	LDL concentration (mol/m ³)
\bar{c}	Intima volume-averaged LDL normalized concentration
C	Thermal capacity (J/kg K)
D	LDL diffusivity (m ² /s)
k	First-order reaction coefficient (1/s)
k_T	Thermal-diffusion coefficient
\bar{K}	Hydraulic permeability (m ²)
\vec{J}	Mass flux (mol/m ² s)
L	Length of the artery (m)
M	Molecular weight (g/mol)

\vec{q}	Heat flux (W/m ²)
p	Hydraulic pressure (mmHg)
r	Radial coordinate (m)
R_g	Universal gas constant (J/mol K)
T	Temperature (K)
u	Velocity vector axial component (m/s)
v	Velocity vector radial component (m/s)
\vec{V}	Velocity vector (m/s)
z	Axial coordinate (m)
z_0	Distance between center of the stenosis and its beginning (m)
z_{st}	Axial coordinate at the center of the stenosis (m)

Greek letters

α	Thermal diffusivity (m ² /s)
δ	Minimum thickness of the stenosis normalized with lumen radius
ε	Porosity
λ	Thermal conductivity (W/m K)
μ	Dynamic viscosity (kg/m s)
ρ	Density (kg/m ³)
σ	Staverman reflection coefficient

Subscripts

0	Entrance condition
eff	Effective property
f	Fluid (plasma) property
w	Wall property
z	Axial component

INTRODUCTION

It is known that cardiovascular diseases (CVD) are the most common causes of death in the world.⁵⁹ In this

Address correspondence to Kambiz Vafai, Department of Mechanical Engineering, University of California, Riverside, CA 92521, USA. Electronic mail: vafai@engr.ucr.edu

category, the atherosclerotic heart disease is the most frequent one.²⁰ An atherosclerotic heart disease is caused by the restriction of a section of an artery, known as stenosis, which causes a reduction of the blood flow. This stenosis is caused by the thickening of the tunica intima. The accumulation of lipids, proteins and fibrous connective tissue in the intima causes the formation of an atherosclerotic plaque. The real cause behind the formation of this plaque is still subject of debate,³³ but what is known is that the oxidation made in the intima by free radicals on the low-density lipoprotein (LDL) promotes the growth of the plaque.²² Indeed, the most accredited theory suggests that monocyte white blood cells penetrate in the tunica intima, transforming into macrophages. The oxidized LDL is absorbed by these macrophages. The high-density lipoprotein (HDL) has the role of removing the LDL from the macrophages. If the HDL is not able to remove all the LDL, foam cells will be formed. Besides, the release of some chemiotactic factors promotes the migration of smooth muscle cells (SMC) from tunica media to intima. These cells engulf the oxidized LDL, generating other foam cells in the tunica intima. The whole process thickens the tunica intima with the generated plaque. Atherosclerotic plaques can be distinguished in stable and unstable forms. In stable plaques, the fibrous cap, which is a layer between the plaque and the lumen, is thick and solid. Unstable plaques are the most dangerous because the fibrous cap is thin and weak and the formation of a thrombus can occur, due to the easier breakage of the fibrous cap.

There are two used methods to describe LDL mass transport through an arterial wall. The first is a method based on experimentation on animals. Meyer *et al.*⁴⁴ studied the effects of pressure on LDL transport through a rabbit aortic wall. Xie *et al.*⁶³ analyzed the influence of LDL concentration polarization and of the flow fields on the localization of an atherosclerosis for rabbits and zebrafishes. The concentration polarization consists of accumulation of solute on a membrane surface.¹⁵ The second method is based on the resolution of transport governing equations within a modeled geometry. According to Yang and Vafai,⁶⁵ Ai and Vafai⁴ and Prosi *et al.*,⁴⁸ three different categories of modeling can be identified. Models of the first category are under the name of wall-free models, in which the arterial wall is replaced by simplified boundary conditions. Wada and Karino⁶¹ used this model to study concentration polarization of LDL at the blood/endothelium boundary. This model is too simplified because it does not take into account the crucial concentration profile along the wall. The second category is characterized by the fluid-wall models, in which the arterial wall is represented by a homogeneous layer. Stangeby and Ethier⁵² used this model to describe oxygen and LDL transport through

this layer. The third category is the most complex, because these consider the heterogeneity of the layers which compose the wall. Usually, four layers, namely endothelium, intima, internal elastic lamina (IEL) and media, are considered in this category. Heterogeneity of the arterial wall is taken into account and each layer of the arterial wall is analyzed in detail.

Sun *et al.*⁵⁵ used a fluid-wall single-layered model to investigate LDL transport for an *in vivo* computed tomographic (CT) image-based human right coronary artery. CT was also used by Kenjereš and de Loor³⁴ to investigate LDL transport within a four-layer wall model, and by Malvè *et al.*⁴² to investigate the effects of a stent placement within a rabbit tracheal wall. Images have been utilized also by Sàez *et al.*⁵⁰ to study the hypertensive growth on a real artery and computer tomography has been used for modeling of an artery (Kiousis *et al.*³⁸ and Auer *et al.*⁸).

Several studies have been performed to set up the physical properties necessary to characterize the multi-layer model. Mostly, these layers are treated as porous media, and properties can be obtained with the support of pore theory or fiber matrix models.^{24,57} Karner and Perktold²⁸ studied the endothelial damage and blood pressure effects on albumin accumulation on the arterial wall, using transport parameters taken from fiber matrix theory for intima and media, and from pore theory for endothelium and IEL. In order to describe the flow field and mass transport phenomena, they used Darcy's law¹⁷ and the volume-averaged stationary convection–diffusion–reaction equation for intima and media, and Staverman–Kedem–Katchalsky³² membrane equations for endothelium and IEL. Prosi *et al.*⁴⁸ have remarked the importance of some experimental data to validate a theoretical estimation. For this purpose, they developed a methodology in which physical parameters are chosen so as to obtain the same LDL concentration profiles of the available experimental data. Because Staverman–Kedem–Katchalsky equations don't take into account effects such as time-dependent phenomena or pulsatile flow, Yang and Vafai⁶⁵ used the porous media theory to study LDL transport across the arterial wall. They used governing equations based on the volume averaging technique. The porous media theory approach was also used by Ai and Vafai,⁴ but their model is based on properties calculated with reference to *in vivo* and *in vitro* measurements, with exact solutions of the concentration field. Porous media theory is also widely used for generic diffusion–advection bio-related problems.^{1,3,53} A detailed comprehensive model was used by Chung and Vafai¹⁰ to study the effects of fluid–structure interactions.

Investigations on macrostructure of the artery were also carried out for a stenosis or a bifurcation by Ai and Vafai,⁴ and by Khakpour and Vafai.³⁵ Ai and

Vafai⁴ demonstrated the effect of a stenosis on the LDL transport. Chung and Vafai¹¹ studied the effects of microstructure in each layer on the stenosis, considering effects of a leaky junction and fibrous cap. They concluded that the microstructure is affected by the presence of the stenosis. However, the evolution of atherosclerotic plaques is still not fully understood.¹⁴

Because of the importance of hyperthermia for the treatment of some diseases like cancer,²¹ it is important to fully understand the effects of induced temperature fields on species transport inside a human body. It is also of interest to see if hyperthermia can be the solution for other diseases, such as atherosclerosis, which may be treated with hyperthermia.¹² Heat could be applied from the interior wall of the artery. Internal heating can occur by means of laser thermal angioplasty, a technique that removes an atheroma *via* heat-induced vaporization. External heating could be applied with a conventional hyperthermia technique, using radiofrequencies or microwaves. Heat transfer interacts with mass transfer *via* thermophoresis, also known as Ludwig-Soret effect. This effect causes a concentration gradient, in the presence of a temperature gradient. Despite a large interest within the research community, this phenomenon still misses a clear explanation.¹⁹ The counter-part of Ludwig-Soret effect is the Dufour effect, which refers to the situation when a concentration gradient affects the temperature field. Many studies were focused on the combined effects between heat transfer and mass transport. It is known that Ludwig-Soret and Dufour effects are not negligible in several situations. In order to fill this gap, few researchers are now working on these coupling effects. Two exhaustive reviews on recent results on Ludwig-Soret effect were made by Platten⁴⁷ and Rahman and Saghir.⁴⁹ The influence of both effects on LDL transport through an arterial wall was investigated by Chung and Vafai,¹² for a healthy artery. However, the impact of a thermal load and heat transfer on a stenosed arterial wall has not been studied in the literature.

In the present study, the impact of a thermal load on a stenosed arterial wall is studied with respect to the thickening of the atherosclerosis plaque, within a comprehensive four-layer model.

MATHEMATICAL MODEL

Anatomy of an Artery

The microscopic anatomy of an artery is shown in Fig. 1. An artery is a blood vessel that delivers blood from the heart to the rest of the body. Starting from the internal part of the artery, the cavity in which

the blood flows is called the lumen. The first layer which is in direct contact with the blood is the tunica intima. The blood-exposed side of the intima is formed by a layer of endothelial cells, aligned and stretched in the direction of the blood flow, forming the endothelium. The endothelium is covered and protected by a structure named glycocalyx. The role of the endothelium is important for fluid filtration, as it acts as a semi-selective barrier between the lumen and the rest of the layers. After the endothelium, there is connective tissue, and a thin layer of elastic tissue, called internal elastic lamina (IEL), which separates the tunica intima from the tunica media, which is the next layer. The tunica media is made of smooth muscle cells and connective tissues. Often, an external elastic lamina separates the tunica media from the next layer, namely tunica adventitia. The tunica adventitia is made of connective tissues, in particular collagen fibers. In this last layer, there are also some capillaries, such as lymphatic vessels and vasa vasorum.

Geometry

Multi-layer Model

The abdominal artery is modeled as a typical long artery, which could be the aorta. The typical length of the computational domain is set up as $L = 22.32$ cm.⁴ Values for the thickness of each layer are taken from literature^{4,10,34,48} and listed in Table 1. We will follow the four-layer model established by Yang and Vafai⁶⁵ and Ai and Vafai.⁴ In addition to the lumen, the four layers are endothelium, intima, IEL and media. In the present work, glycocalyx effects are neglected, as often happens in literature,^{34,65} because of its negligible thickness.⁵⁸ However, it has been found that the health of the endothelial glycocalyx layer has a role in LDL infiltration through the arterial wall.⁴⁰ As such, the tunica adventitia is substituted with a boundary condition. It has been shown that, if transport of LDL through vasa vasorum is neglected, the concentration at the media/adventitia interface is only slightly influenced by the applied boundary condition.^{48,65}

Stenosis Model

Different shapes of stenosis have been considered by researchers.⁴³ Seeley and Young⁵¹ carried out a study of blunt-ended hollow plugs with a rectangular shape, in order to study the effects of geometrical characteristics on pressure drop through an arterial stenosis. Jung *et al.*²⁶ numerically studied characteristics of pulsatile flow using a trapezoidal stenosis profile. Auer *et al.*⁷ presented a 3D construction of tissue components in an artery with an atherosclerotic plaque. Cilla

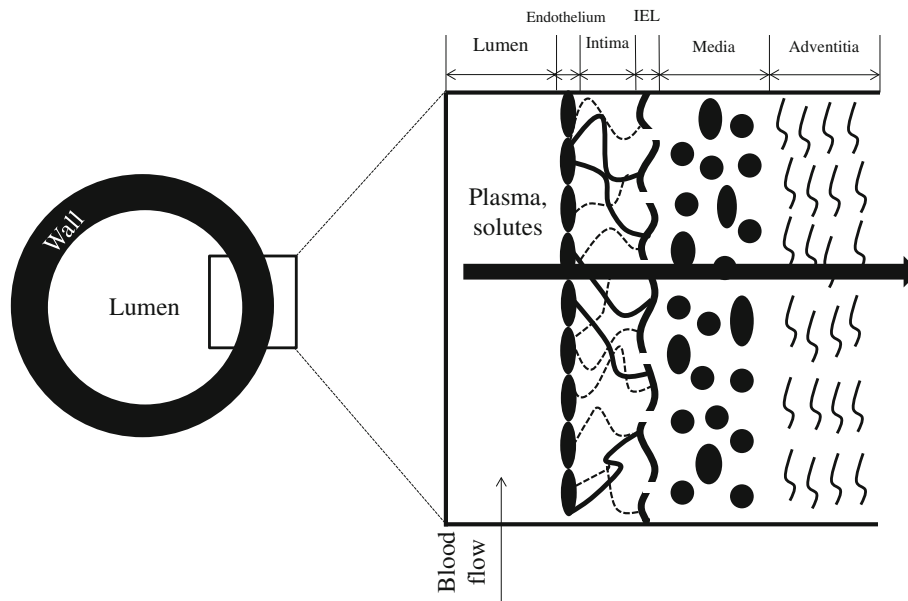


FIGURE 1. Display of different layers constituting the arterial wall.

TABLE 1. Properties within each domain, from Chung and Vafai.¹⁰

Property	Lumen	Endothelium	Fibrous cap	Intima	IEL	Media
Thickness (μm)	3,100	2	65	10	2	200
Density ρ (kg/m^3)	1.07×10^3	1.057×10^3	–	1.057×10^3	1.057×10^3	1.057×10^3
Viscosity μ ($\text{kg}/\text{m s}$)	3.7×10^{-3}	0.72×10^{-3}	–	0.72×10^{-3}	0.72×10^{-3}	0.72×10^{-3}
Porosity ε	–	0.0005	–	0.983	0.002	0.258
Hydraulic permeability K (m^2)	–	3.22×10^{-21}	–	2×10^{-16}	4.392×10^{-19}	2×10^{-18}
Effective diffusivity D_{eff} (m^2/s)	2.87×10^{-11}	5.7×10^{-18}	$4.5 \times 10^{-13\text{a}}$	5.4×10^{-12}	3.18×10^{-15}	5×10^{-14}
Reflection coefficient σ (1)	–	0.9888	–	0.8272	0.9827	0.8836
Reaction coefficient k (1/s)	0	0	0	0	0	3.197×10^{-4}
Thermal diffusivity α (m^2/s)	–	$1.42 \times 10^{-7\text{b}}$				

^aFibrous cap properties are taken from Hossain *et al.*²³

^bThermal properties are taken from Duck¹⁸ and Kolios *et al.*³⁹

*et al.*¹³ investigated the role of the morphology on plaque rupture. An approach for segmentation of an artery with an atherosclerotic plaque has been presented by Yang *et al.*⁶⁴ However, most realistic and commonly used geometries are the axisymmetric bell-shaped stenosis⁴⁵ and the axisymmetric cosine-shaped stenosis.^{27,66} In this work, the generalized axisymmetric stenosed shape proposed by Young and Tsai,⁶⁶ Ai and Vafai⁴ and Chung and Vafai¹¹ is utilized. The geometry of the stenosis is represented in Fig. 2. The shape of the axisymmetric stenosis is determined by the following equation:

$$\frac{r}{R} = 1 - \frac{\delta}{2R} \left[1 + \cos \frac{\pi(z - z_{\text{st}})}{z_{\text{st}}} \right] \quad (1)$$

for $-z_0 \leq (z - z_{\text{st}}) \leq z_0$

In Eq. (1), r is the radial coordinate, z is the axial coordinate, subscripts st and 0 respectively refer to the axial coordinate at the center of the stenosis (maximum

thickening) of the stenosis, and to the distance between the center of the stenosis and the coordinate z_{st} , R is the radius of the lumen, and δ is a dimensionless parameter that takes into account the severity of the stenosis.

From the geometrical point of view, the parameter that takes into account the severity of a stenosis is the area reduction A of a stenosis, defined by:

$$A = 1 - \left(\frac{r(z_{\text{st}})}{R} \right)^2 = 1 - (1 - \delta)^2 \quad (2)$$

In order to take into account different levels of stenosis severity, in the present study values of $\delta = 1/4$ and $1/2$ are considered. Following the classification of stenosis provided by Cullen and Hill¹⁶ these two values of δ imply values of the area reduction A , in percentage, of 43.75% (mild stenosis) and 75% (severe stenosis), respectively.

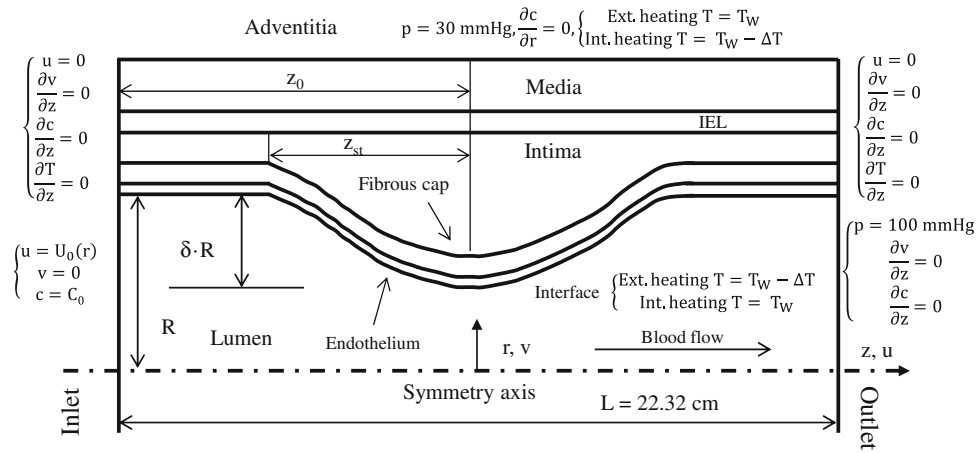


FIGURE 2. Detailed geometrical attributes and boundary conditions for an artery in the presence of stenosis.

In analyzing the effect of stenosis, the fibrous cap has to be taken into account. A fibrous cap is made of collagen fibers and smooth muscle cells, and it lies between endothelium and thickened intima. Hossain *et al.*²³ reported that a fibrous cap is considered as thin if its thickness is less than $65 \mu\text{m}$. Usually, a thin fibrous cap translates into an unstable plaque formation, and as such is more dangerous than a stable one. In this study, a fibrous cap is modeled with a thickness of $65 \mu\text{m}$.

GOVERNING EQUATIONS

In analyzing the thermal effects on the stenosis, we have utilized the following well established results based on prior research works:

- In the lumen region, blood is considered as an incompressible and Newtonian fluid,² if the artery is large or medium³⁶;
- Pulsatile flow effects are considered to be negligible^{10,65};
- Flow is assumed to be laminar and fully developed at the inlet of the lumen,
- Osmotic pressure effects on the velocity in the arterial wall are considered to be negligible^{4,65};
- Fluid and solid phases through the arterial wall are considered to be in thermal equilibrium.^{5,6}

Lumen

Based on the above results, the governing equations for the blood within the lumen region are prescribed by:

$$\nabla \cdot \vec{V} = 0 \quad (3a)$$

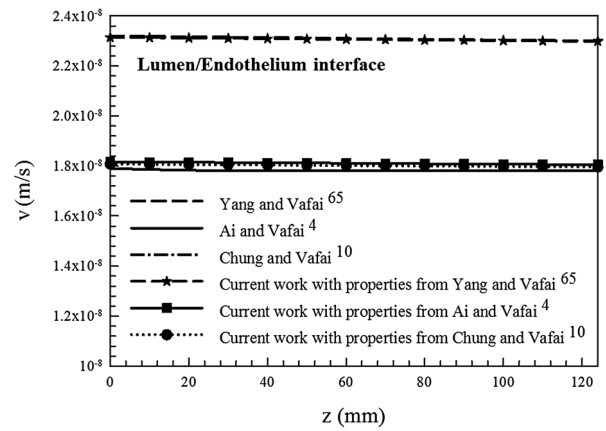


FIGURE 3. Comparison of the filtration velocity obtained from the current model with other pertinent works in the literature.

$$\nabla p = \mu_f \nabla^2 \vec{V} \quad (3b)$$

$$\vec{V} \cdot \nabla c = D_f \nabla^2 c \quad (3c)$$

where \vec{V} is the velocity vector, p the pressure, μ_f the plasma viscosity, c the concentration and D_f the diffusion coefficient for the fluid.

Arterial Wall

The total diffusion mass flux \vec{J} , accounting for the Ludwig-Soret effect,^{9,12,31,62} is given by:

$$\vec{J} = -D_{\text{eff}} \nabla c - \frac{k_T \rho_f D_{\text{eff}}}{M_f T} \nabla T \quad (4)$$

where D_{eff} is the effective diffusivity, k_T thermal-diffusion coefficient and ρ_f and M_f are density and molecular weight of the plasma, respectively, and T is the temperature. The counterpart of the Ludwig-Soret effect for the heat transfer is the Dufour effect, which is taken into

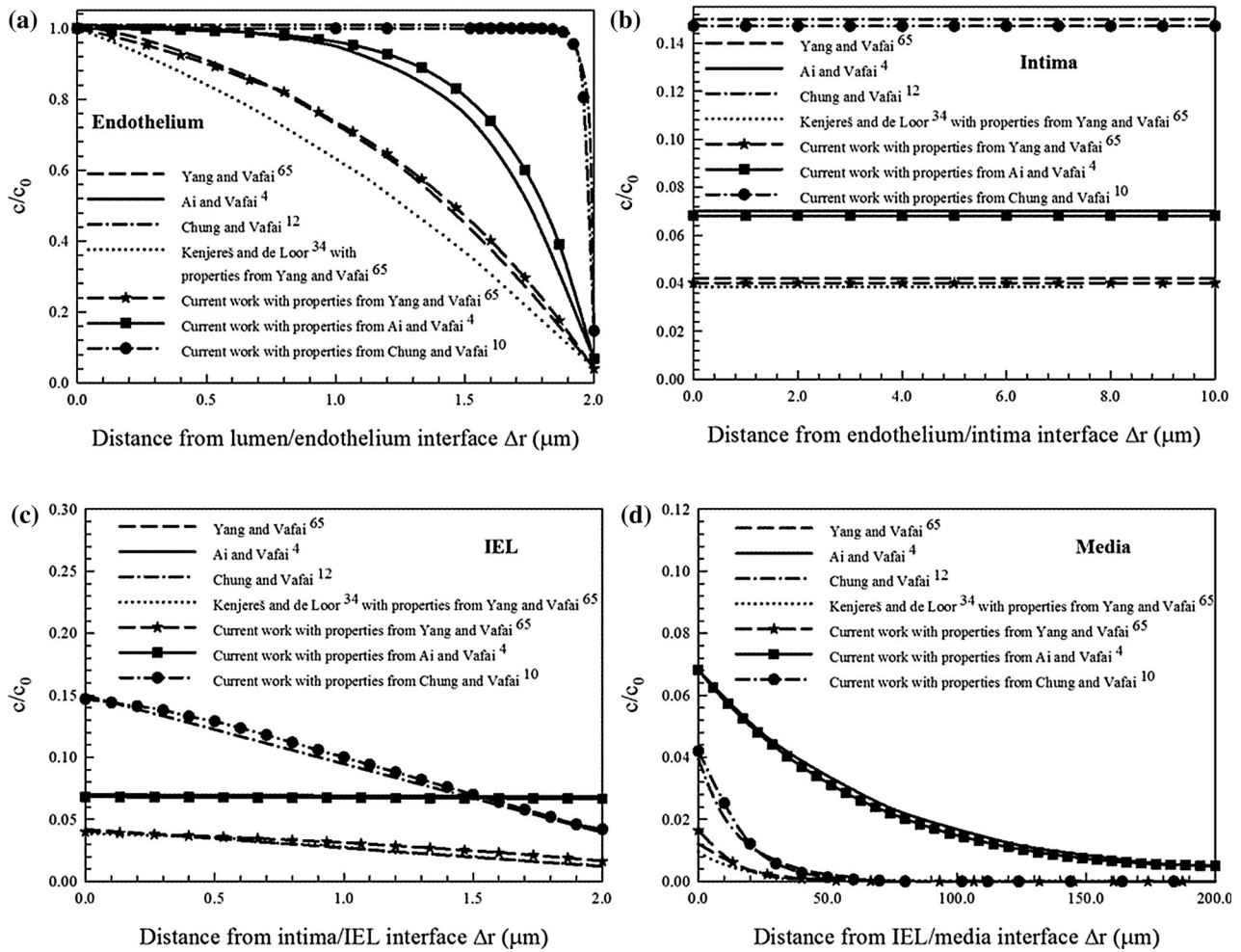


FIGURE 4. Comparison of the LDL concentration levels across the artery obtained by the current model with other pertinent works in the literature for (a) endothelium; (b) intima; (c) IEL and (d) media.

account in the present study. Heat flux \vec{q} is described by Fourier law, taking into account Dufour effect^{9,12,31,62}:

$$\vec{q} = -\lambda_{\text{eff}} \nabla T - \frac{R_g T k_T \rho_f D_{\text{eff}}}{M_f c} \nabla c \quad (5)$$

where λ_{eff} is the effective thermal conductivity, and R_g represents the universal gas constant. Dufour effect has been modeled as in Chung and Vafai.¹² We utilize Darcy-Brinkman equation for the flow, diffusion-convection-reaction equation while taking into account Staverman-Kedem-Katchalsky membrane transport equation for the species transport, and the energy conservation equation for the thermal transport:

$$\nabla \cdot \vec{V} = 0 \quad (6a)$$

$$\nabla p = \mu_{\text{eff}} \nabla^2 \vec{V} + \frac{\mu_{\text{eff}}}{K} \vec{V} \quad (6b)$$

$$(1 - \sigma) \vec{V} \cdot \nabla c = D_{\text{eff}} \nabla^2 c + \frac{k_T \rho_f D_{\text{eff}}}{M_f T} \nabla^2 T - kc \quad (6c)$$

$$\vec{V} \cdot \nabla T = \alpha_{\text{eff}} \nabla^2 T + \frac{R_g T k_T D_{\text{eff}}}{C_T M_f c} \nabla^2 c \quad (6d)$$

The term μ_{eff} represents the effective viscosity, which is the ratio between the plasma viscosity and porosity.⁶⁰ The selective rejection of species by membranes is taken into account with the dimensionless term σ , i.e., Staverman filtration coefficient. In the media, smooth muscle cells and macrophages take LDL to form foam cells. This physical phenomenon can be approximated by an irreversible first-order reaction,¹⁰ where k represents the first-order reaction coefficient. In the energy equation, α_{eff} represents the effective thermal diffusivity and C_T the plasma's thermal capacity.

Boundary Conditions

The pertinent, comprehensive boundary conditions for the arterial transport which have been used in the present study are illustrated in Fig. 2. For various

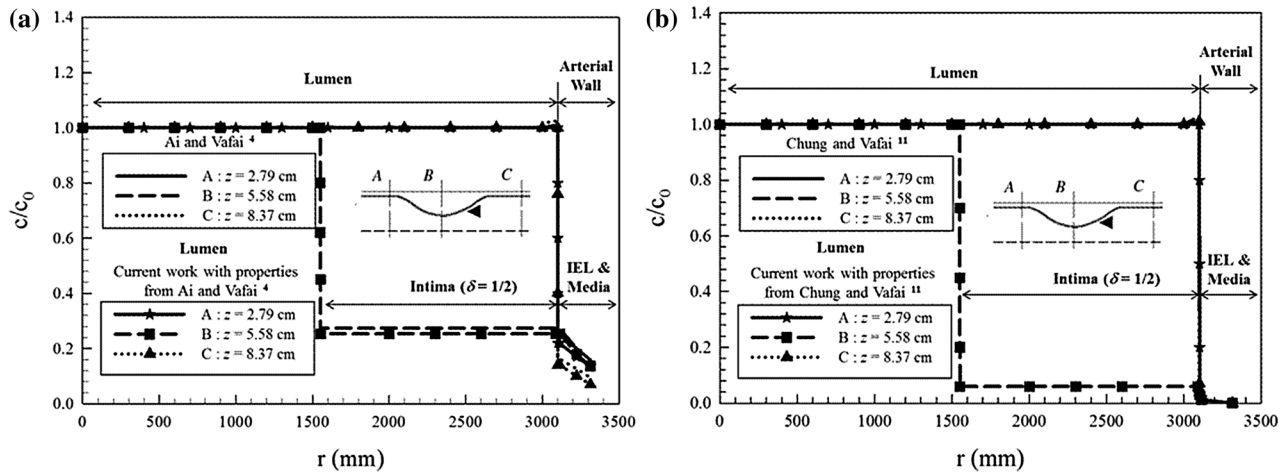


FIGURE 5. Comparison of the LDL concentration levels across a stenosed artery with (a) Ai and Vafai⁴ and (b) Chung and Vafai,¹¹ with $z_{st} = 5.58$ cm and $\delta = 1/2$.

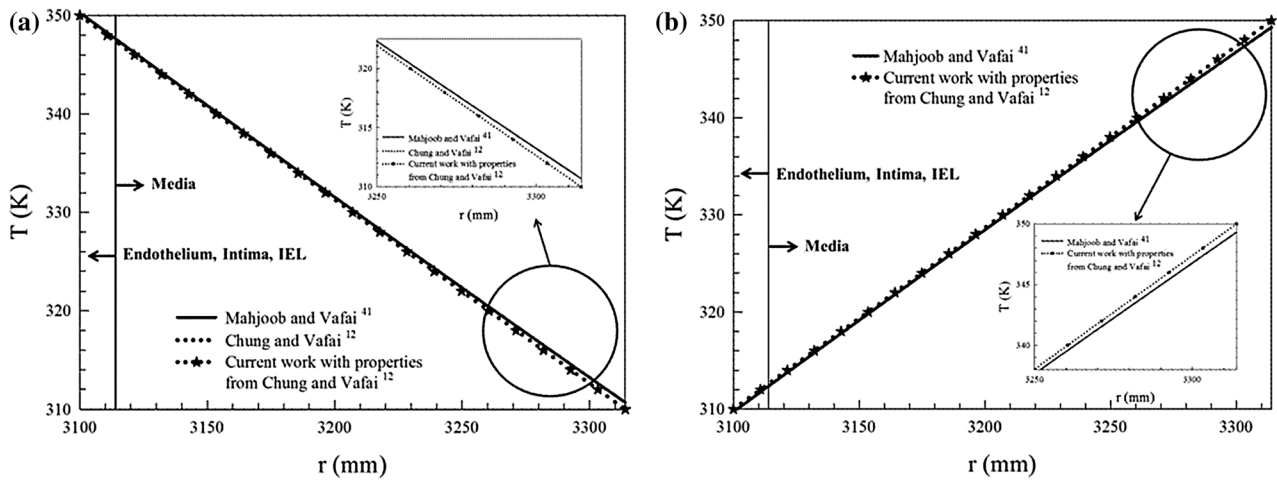


FIGURE 6. Comparison of hyperthermia induced temperature profiles along the arterial wall obtained by the current model with the analytical results of Mahjoob and Vafai,⁴¹ (a) internal heating and (b) external heating.

configurations relative to the comparison of our model with the literature data, boundary conditions are the same. Velocity at the inlet of the lumen is considered to be parabolic and fully developed flow:

$$u = u_0 \left(1 - (r/R)^2\right) \quad \text{for } z = 0, \quad 0 \leq r \leq R \quad (7)$$

where u is the z -component of the velocity, and the maximum velocity u_0 is equal to 0.338 m/s.^{11,29}

The inlet LDL concentration c_0 is taken as 28.6×10^{-3} mol/m³,^{11,30} which is a value relative to a healthy human. The pressure p is set as 30 mmHg at media/adventitia interface,^{4,10,12,65} and 100 mmHg at the lumen outlet. This means that the transmural pressure is 70 mmHg, a value which is a little bit less than physiological pressure.⁴⁴ Since this is the mostly

used value in literature, it is remarked that what is important is the transmural pressure, which is the driving force for the lateral flow. Indeed, a sensitivity analysis on the media-adventitia interface boundary condition was developed by Yang and Vafai,⁶⁵ showing that this is the most realistic boundary condition. The important effects of pressure on arterial failure have been discussed in Khamdaengyodtai *et al.*³⁷ Considering 310 K as the temperature of an isothermal arterial wall under normal conditions, the imposed interface temperature T_w for both internal and external heating has been chosen as 330 and 350 K. These values of temperature can be obtained with laser thermal angioplasty for internal heating, or with radiofrequency/microwave hyperthermia for external heating. According to the tissue thermal damage

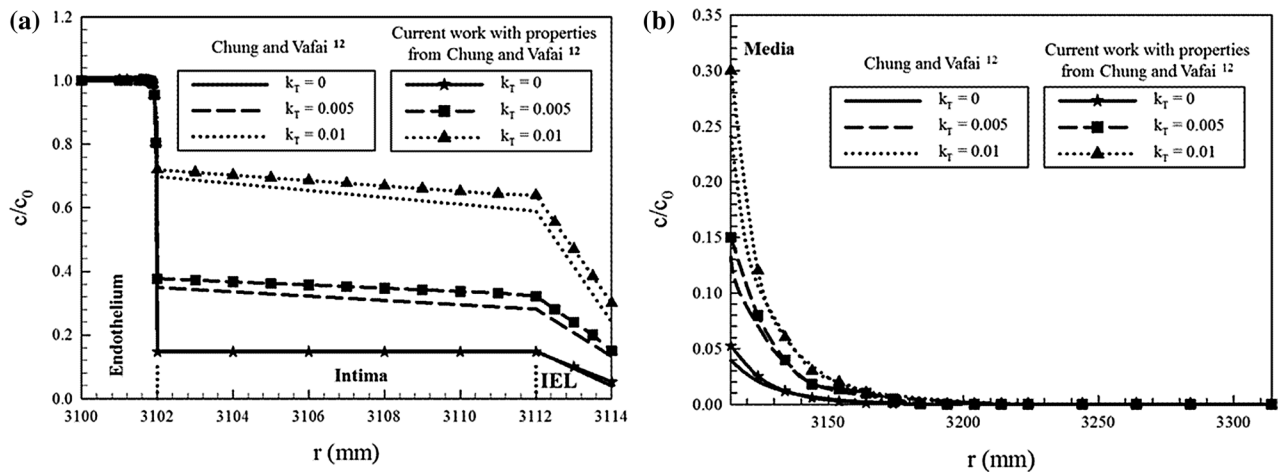


FIGURE 7. Comparison of hyperthermia effects on LDL concentration across a normal artery obtained with the current model with Chung and Vafai¹² for (a) endothelium, intima and IEL; (b) media.

classification by Steiner,⁵⁴ tissues are not irreversibly damaged if the exposition time is short. In case of a longer exposition, coagulation can occur. As such, the temperature difference ΔT between the opposite surfaces of the arterial wall are respectively 20 and 40 K. Continuity of the mass between different layers, incorporating Staverman reflection effects, is guaranteed by the following:

$$\left[(1 - \sigma)vc - D_{\text{eff}} \frac{\partial c}{\partial r} \right]_{+} = \left[(1 - \sigma)vc - D_{\text{eff}} \frac{\partial c}{\partial r} \right]_{-} \quad (8)$$

where v represents the filtration velocity, relative to the flow that is penetrating inside the arterial wall in the radial direction.

Properties Utilized Within the Models

Assignment of the property values that are utilized within the present model is not a trivial task. In our work, the properties of the four-layer arterial wall are in general taken after Chung and Vafai.¹⁰ Transport properties were obtained using electrical analogy starting from experimental results often from rabbit aortas.⁴⁸ Geometrical properties are referred to human aorta. Thermal properties are obtained for muscle tissue. However, we have also used properties from Yang and Vafai⁶⁵ and Ai and Vafai⁴ in comparing our results with their models. It should be mentioned that the computational schemes utilized in Yang and Vafai⁶⁵ and Ai and Vafai⁴ were entirely different than the scheme used in this work. Fibrous cap properties are described with reference to Hossain *et al.*²³ Thermal properties such as thermal conductivity and heat transfer capacity at constant pressure are taken from

Duck¹⁸ and Kolios *et al.*³⁹ These properties are displayed in Table 1.

METHODOLOGY

Mesh Setup

Governing equations with appropriate boundary conditions are solved with a finite element based software, namely, Comsol Multiphysics, with a root-mean square (RMS) residual of 10^{-6} . It has been checked that the solution is not significantly changing when the residual value is lower. For the validation of the cases in which there is not a stenosis, a rectangular mesh has been used. For the validation cases in which there is a stenosis, and for the case relative to a stenosis in presence of thermal effect, a triangular mesh has been used. All the meshes, as well as the geometries, were generated based on the aforementioned criteria.

Validation

Comprehensive and rigorous validation of our model was accomplished with the few cases that were available in the literature. The validation has been made demonstrating that, if physical properties from different papers are used in our model, results were the same as the ones reported in the mentioned papers. The transversal section that has been considered in the plot of variables along the radius is half of the artery's cross sectional domain.

For an isothermal straight artery, comparisons are reported in Figs. 3 and 4. For filtration velocity results in Fig. 3, comparisons have been carried out with papers of Yang and Vafai,⁶⁵ Ai and Vafai,⁴ Chung and

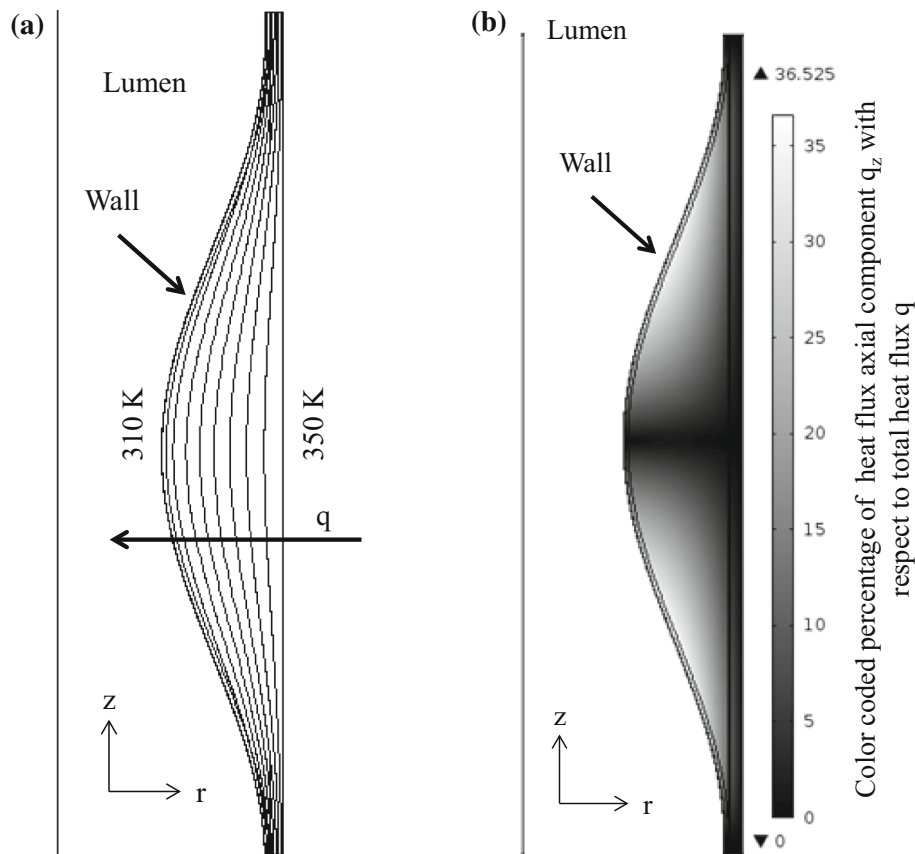


FIGURE 8. (a) Isothermal contours with external heating and $\Delta T = 40$ K; (b) Axial component of heat flux q_z influence on the total heat flux q .

Vafai.¹⁰ It is remarked that the solution schemes used in these works are entirely different from the present work. Figure 4 shows comparisons with the dimensionless concentration distribution, for endothelium, intima, IEL and media. In addition to comparing the results with Yang and Vafai,⁶⁵ Ai and Vafai,⁴ Chung and Vafai,^{10,12} numerical results for a realistic carotid artery bifurcation from Kenjereš and de Loor³⁴ are also compared. It should be noted that Kenjereš and de Loor³⁴ have utilized, for their numerical model, properties from Yang and Vafai.⁶⁵ As can be seen in Figs. 3 and 4, an excellent agreement can be observed between our results and prior works which were obtained with different numerical schemes.

Comparisons of the concentration profiles for the isothermal stenosed artery are reported in Fig. 5. Once again there is an excellent match between the present results and literature data. The insignificant differences between results from Ai and Vafai⁴ and Chung and Vafai,¹¹ and our results obtained using same properties of the same two cited papers, are due to the use of different models and solution schemes in these works. From the physical point of view, results from Ai and Vafai⁴ and Chung and Vafai¹¹ are strongly influenced

by the use of different properties. Observing Figs. 4 and 5, we notice that for Ai and Vafai⁴ concentration in the intima increases with the stenosis, opposite from what is happening in Chung and Vafai.¹¹ To understand this difference, we first remark that mass Peclet numbers in the endothelium are 70 if properties from Chung and Vafai¹¹ are used, and 5 if properties from Ai and Vafai⁴ are used. This means that in the first case contribution from advection is higher than in the second case. The presence of the stenosis let the wall shear stresses to be locally higher. It has been demonstrated that higher shear stresses means lower LDL concentration.^{46,56} This means that concentration in the intima is reduced if the problem is advection-dominated, due to the substantial effect of shear stresses. On the other hand, the shear stresses effect on LDL becomes lower if the transport in the endothelium is reduced. Indeed, mass Peclet numbers are respectively around 70 and 5. This explains why concentration in the intima decreases when properties from Chung and Vafai¹¹ are used. On the other hand, concentration in the intima increases when properties from Ai and Vafai⁴ are used. This is because diffusion has a more important role than the wall shear stresses,

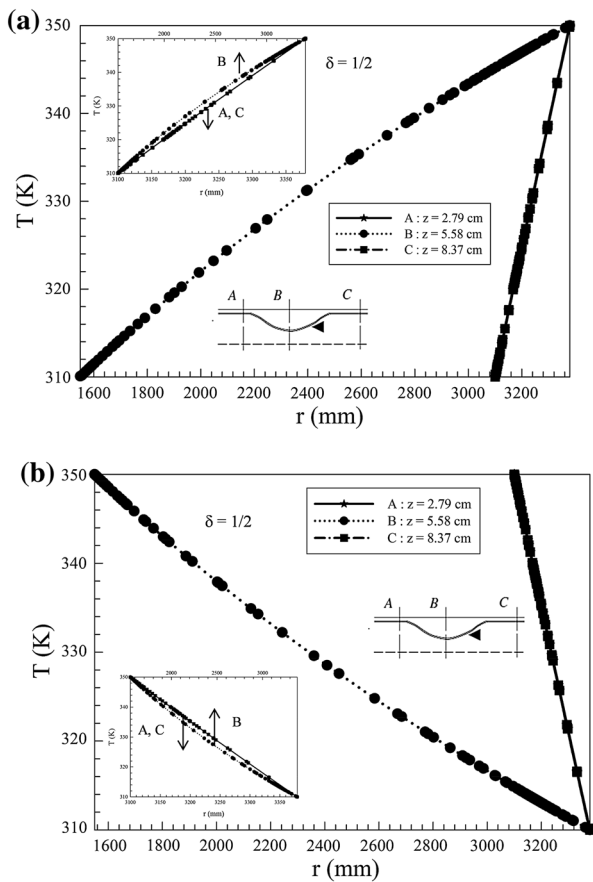


FIGURE 9. Hyperthermia induced temperature profiles at different axial locations with $z_{st} = 5.58$ cm and $\delta = 1/2$, for (a) external heating and (b) internal heating. Effects of changing slopes of the curves is remarked within the smaller figure insert within Fig. 9.

with less influence on LDL transport, and concentration increases because the region of the wall with the lowest diffusivity (intima) is an order of magnitude larger than the case with a straight artery.

With respect to the thermal effects, the temperature profiles through the arterial wall for the present study are compared with the analytical solution of Mahjoob and Vafai⁴¹ and the results given in Chung and Vafai,¹² for both external and internal heat loads. These comparisons are presented in Fig. 6. It has to be mentioned that results for external heating are available in literature only for Mahjoob and Vafai.⁴¹ Once again an excellent match between our results and those of the cited references is observed.

Results for a straight artery under hyperthermia conditions, considering Ludwig-Soret effect, are displayed in Fig. 7. As can be seen, all our results from Figs. 3, 4, 5, 6 and 7 compare very well with all of the cited works. Furthermore, results from Ai and Vafai⁴ were in good agreement with the experimental data from Meyer *et al.*⁴⁴

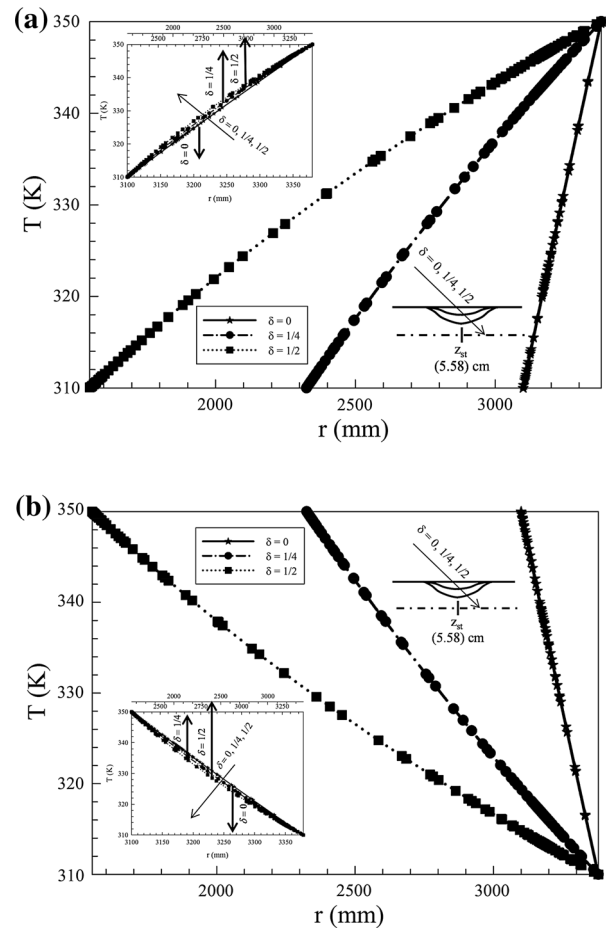


FIGURE 10. Atherosclerotic plaque thickening effects on the hyperthermia induced temperature profiles, (a) external heat load and (b) internal heat load. Effects of changing slopes of the curves with δ is highlighted in the smaller figure insert and is remarked within the smaller figure insert within Fig. 10.

RESULTS AND DISCUSSION

Heat-Induced Gradients Effects on LDL Transport and Accumulation on a Stenosed Artery

Isothermal contours and the influence of the heat flux axial component q_z on the total heat flux q for external heating are shown in Fig. 8. Thermophysical properties are considered to be uniform and homogeneous.^{18,39} Considering the atherosclerotic plaque region, it can be seen that the heat flux becomes unidirectional only in the largest section of the plaque. The regions near the lumen/endothelium interface have the largest influence on the axial heat flux. In the lower section, the radial temperature gradients are substantially lower in the presence of stenosis as compared to a region where it is absent. As reported by Chung and Vafai,¹² and as seen in Fig. 9, the temperature profile is almost linear in regions where stenosis is not encountered. This effect can further be justified by the value of

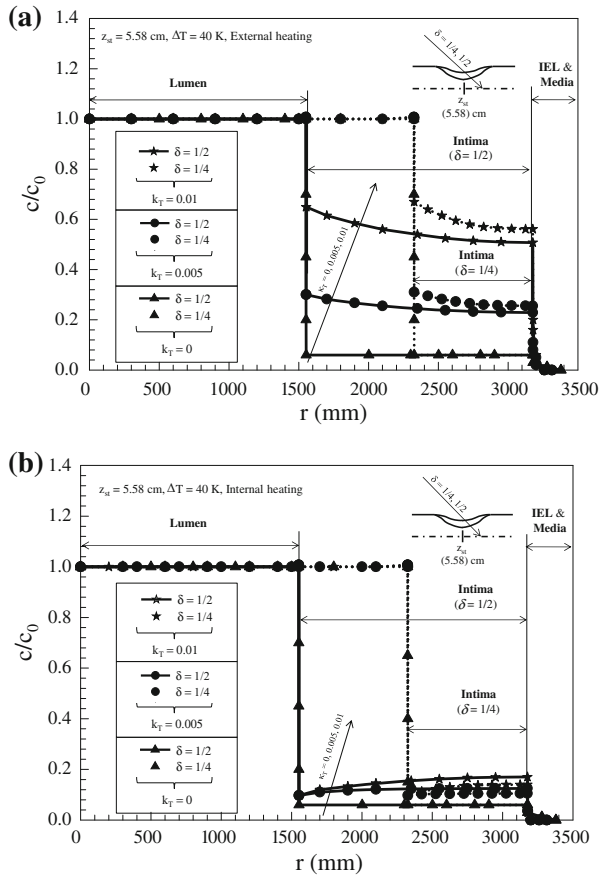


FIGURE 11. Hyperthermia and atherosclerotic plaque thickening effects on LDL concentration across the arterial wall, for $z_{st} = 5.58$ cm and $\Delta T = 40$ K, for (a) external heating and (b) internal heating.

thermal Peclet number, which is of order of $O(10^{-5})$ in regions where stenosis is not encountered, as compared to an order of $O(10^{-4})$, in regions where it is encountered. In the lowest section, the mono-dimensional profile is less linear. In this section, the thermal Peclet number is of the order of $O(10^{-4})$, and the thickness in meters of the wall is of the order of $O(10^{-4})$, for both $\delta = 1/2$ and $1/4$. It is common in literature to classify a physical problem to be advection-dominated when Peclet number is significantly higher than 1. The review by Huysmans and Dassargues²⁵ report that advection can be negligible for Peclet lower than 1. Under these conditions, advection is negligible in the present work. Effects of changing slopes of the curves is remarked within the smaller figure insert within Fig. 9. For larger δ 's, i.e., thicker walls, the non-linearity attributes becomes more prominent as seen in Fig. 10. The case with $\delta = 0$ is relative to the absence of atherosclerotic plaque. The fibrous cap is not included in this model. Indeed, the fibrous cap is a layer of fibrous connective tissue, which can be found only in atherosclerotic

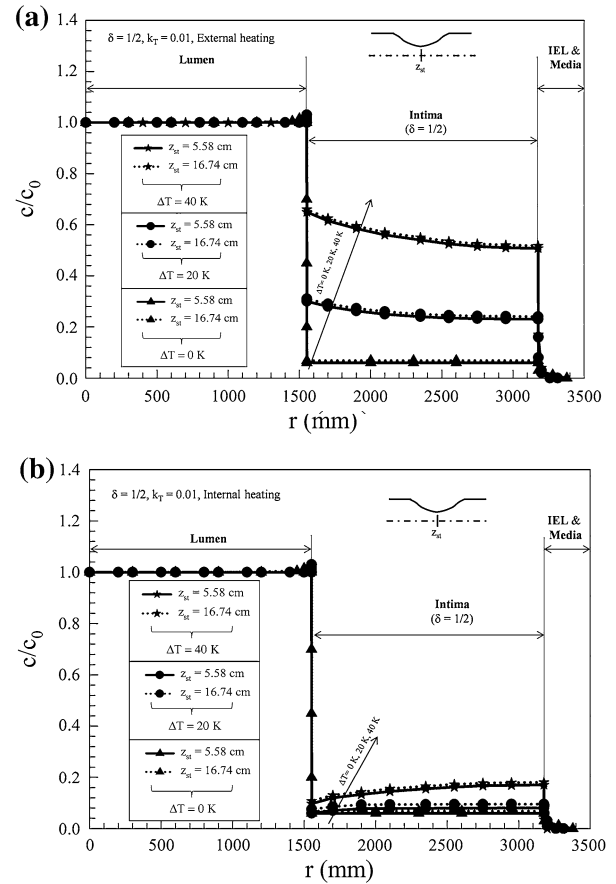


FIGURE 12. Hyperthermia load and axial atherosclerotic plaque formation effects on LDL concentration across the arterial wall, for $\delta = 1/2$ and $k_T = 0.01$, with (a) external heating and (b) internal heating.

plaques. It should be noted that Chung and Vafai¹² have clearly established that the Dufour effects are negligible and as such these effects will not be considered in the present work.

Hyperthermia Load and Axial Atherosclerotic Plaque Formation Effects on LDL Concentration Levels

Effects of hyperthermia on LDL transport through an arterial wall are manifested through Ludwig-Soret effect. As seen in Eq. (4), the thermo-diffusion coefficient, k_T , plays an important role in expressing the thermal effects on the species mass diffusion. Chapman and Cowling⁹ and Wakeham *et al.*⁶² reported that normally k_T is equal or less than 0.01. However, since LDL is a heavier chained molecule, its k_T value is expected to be lower. For this reason, in the present study, values of $k_T = 0.005$ and 0.01 are considered.

Effects of thermo-diffusion coefficient k_T and intima thickening δ are reported in Fig. 11, for both external

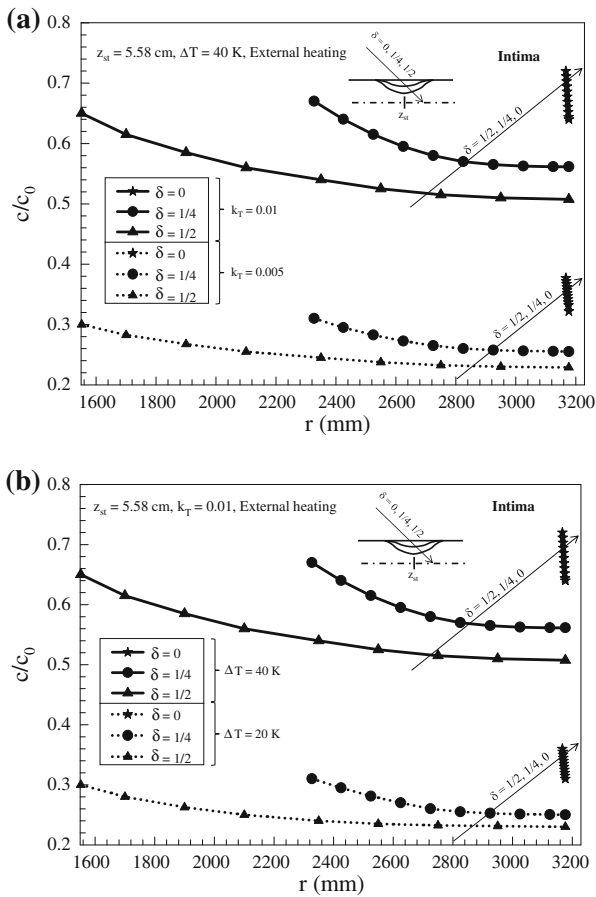


FIGURE 13. Effects of heating loads and severity of stenosis on the LDL concentration levels as compared to a healthy artery ($\delta = 0$), for (a) $k_T = 0.005$ and 0.1 , and (b) $\Delta T = 20$ and 40 K.

and internal heating, at a given axial position z_{st} and ΔT . For both external and internal heating, an increase in k_T increases the general level of LDL concentration, especially in the crucial intima layer, in terms of absolute values and the slope of LDL concentration curve. For internal heating case, Ludwig-Soret effect in general has a lesser influence on mass transport, as compared to the external hyperthermia case.

Physical reasons are described in the following. In a generic solution, Ludwig-Soret effect lets the solute to migrate from the hot zone to the cold zone. In our case, for external heating, particles are migrating from media/adventitia interface to lumen/endothelium interface and vice versa for internal heating. This justifies the different trend of the curves between external and internal heating cases. Furthermore, it appears that external heating affects LDL transport more than internal hyperthermia. The reason for this can be substantiated from Eq. (4). For external heating, the second term on the right sides contributes to an increase in the mass flow \vec{J} more than for the case of

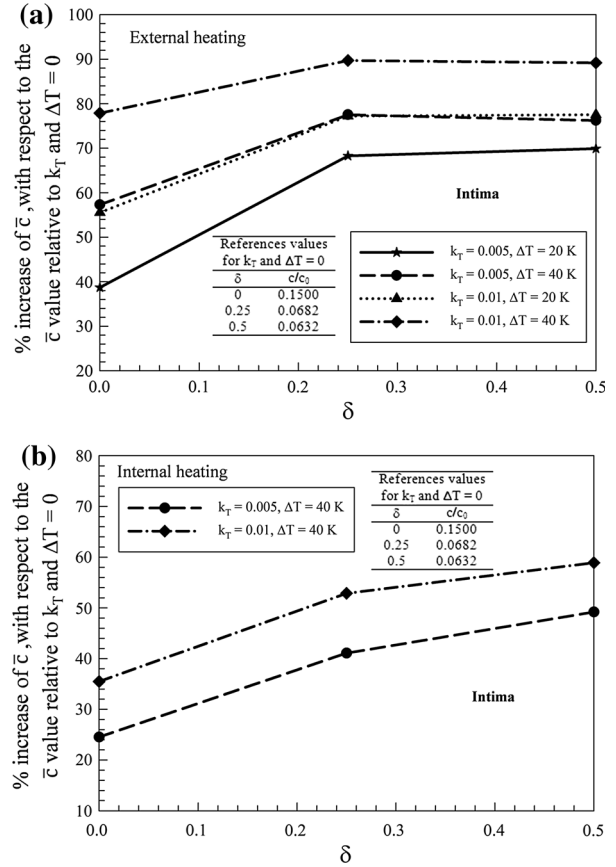


FIGURE 14. Normalized concentration \bar{c} percentage increase in intima subject to different hyperthermia conditions for (a) external heating and (b) internal heating. Fixed a δ value, the percentage increase is calculated with respect to the case with k_T and $\Delta T = 0$.

internal heating. It has also to be noticed that the absolute levels of temperature T play a role. For example, in the tunica intima, for the external heating temperature levels are lower than the ones for internal heating. Observing Eq. (4), we conclude that lower temperature levels contribute to enhance the mass flux \vec{J} . Effects of the plaque axial location on LDL transport during hyperthermia are displayed in Fig. 12. It can clearly be seen that the axial location of the stenosis formation has a negligible effect on the LDL concentration levels. Figure 12 also clearly establishes the enhanced LDL concentration for higher hyperthermia loads. Furthermore, an external hyperthermia load has a larger impact in increasing the LDL concentration levels within the intima region, as compared to an internal heat load, under the same conditions, as seen in Fig. 11.

Differences in LDL concentration in the tunica intima for different stenosis severity are highlighted in Fig. 13. As previously reported, the model with $\delta = 0$ doesn't consider the fibrous cap. It is shown that a

stenosis severity effect is substantial. A maximum difference of about 21% in LDL concentration has been found between $\delta = 0$ and $1/2$, for $z_{st} = 5.58$, $\Delta T = 40$ K and $k_T = 0.01$, at the exterior intima/IEL interface. It is also shown that as the severity of the stenosis increases the non-linearity of the presented concentration distributions increases.

Effects of LDL Accumulation in the Intima Layer due to Hyperthermia

Accumulation of LDL in the intima has also been analyzed. Intima volume-averaged LDL normalized concentration \bar{c} is used as the comparison parameter for different cases. Results are reported in Fig. 14, in terms of the normalized concentration \bar{c} percentage increase, for both external and internal heat loads. Each percentage increase of \bar{c} in the presence of a heat load is calculated with respect to its corresponding case for $\delta = 0, 1/4$ and $1/2$, without hyperthermia. Reference values for LDL normalized concentration c/c_0 , used for each δ value, are reported in the same Fig. 14. It can be seen that hyperthermia effects on intima volume-averaged LDL normalized concentration \bar{c} increases with the thickening of the stenosis and becomes more pronounced with an increase in k_T and ΔT . As can be seen, the enhancement effect is more pronounced for external heat loads.

CONCLUSIONS

Hyperthermia effects on LDL transport through an arterial wall in the presence of an atherosclerotic plaque were rigorously established in the present study. It is shown that the temperature gradients induced by hyperthermia are substantially lower in the presence of stenosis as compared to a location where it is absent.

Atherosclerotic plaque thickening effects on the hyperthermia induced thermal profiles and LDL concentration levels across the arterial wall, for both external and internal loads, are established. Further, hyperthermia effects for internal and external heat loads at different stenosis axial locations are established. It is shown that while the hyperthermia's load level has a substantial effect in increasing the LDL accumulation level, particularly for an external load, the axial location of the stenosis formation has a negligible effect on the LDL concentration level. Our model and results without stenosis or without hyperthermia were validated, the authors remark that there is a lack of experimental data in literature in this area.

ACKNOWLEDGMENTS

The financial support by UniNA and Compagnia di San Paolo, through Programme STAR, is greatly appreciated.

CONFLICT OF INTEREST

There is no conflict of interest. This manuscript has not been submitted to anywhere else.

REFERENCES

- ¹Abraham, J. P., E. M. Sparrow, J. M. Gorman, J. R. Stark, and R. E. Kohler. A mass transfer model of temporal drug deposition in artery walls. *Int. J. Heat Mass Tran.* 58:632–638, 2013.
- ²Abraham, J. P., E. M. Sparrow, and R. D. Lovik. Unsteady, three-dimensional fluid mechanic analysis of blood flow in plaque-narrowed and plaque-free arteries. *Int. J. Heat Mass Tran.* 51:5633–5641, 2008.
- ³Abraham, J. P., J. R. Stark, J. M. Gorman, E. M. Sparrow, and R. Kohler. A model of drug deposition within artery walls. *J. Med. Dev.* 7:020902, 2013.
- ⁴Ai, L., and K. Vafai. A coupling model for macromolecule transport in a stenosed arterial wall. *Int. J. Heat Mass Tran.* 49:1568–1591, 2006.
- ⁵Alazmi, B., and K. Vafai. Analysis of fluid flow and heat transfer interfacial conditions between a porous medium and a fluid layer. *Int. J. Heat Mass Tran.* 44:1735–1749, 2001.
- ⁶Amiri, A., and K. Vafai. Analysis of dispersion effects and non-thermal equilibrium, non-Darcian, variable porosity incompressible flow through porous media. *Int. J. Heat Mass Tran.* 37:939–954, 1994.
- ⁷Auer, M., R. Stollberger, P. Regitnig, F. Ebner, and G. A. Holzappel. 3-D reconstruction of tissue components for atherosclerotic human arteries using ex vivo high-resolution MRI. *IEEE T. Med. Imaging* 25:345–357, 2006.
- ⁸Auer, M., R. Stollberger, P. Regitnig, F. Ebner, and G. A. Holzappel. In vitro angioplasty of atherosclerotic human femoral arteries: analysis of the geometrical changes in the individual tissues using MRI and image processing. *Ann. Biomed. Eng.* 38:1276–1287, 2010.
- ⁹Chapman, S., and T. G. Cowling. *The Mathematical Theory of Non-uniform Gases: An Account of the Kinetic Theory of Viscosity, Thermal Conduction and Diffusion in Gases.* Cambridge: Cambridge University Press, p. 431, 1952.
- ¹⁰Chung, S., and K. Vafai. Effect of the fluid-structure interactions on low-density lipoprotein transport within a multi-layered arterial wall. *J. Biomech.* 45:371–381, 2012.
- ¹¹Chung, S., and K. Vafai. Low-density lipoprotein transport within a multi-layered arterial wall: effect of the atherosclerotic plaque/stenosis. *J. Biomech.* 46:574–585, 2013.
- ¹²Chung, S., and K. Vafai. Mechanobiology of low-density lipoprotein transport within an arterial wall-impact of hyperthermia and coupling effects. *J. Biomech.* 47:137–147, 2014.
- ¹³Cilla, M., E. Peña, and M. A. Martinez. 3D computational parametric analysis of eccentric atheroma plaque: influence

- of axial and circumferential residual stresses. *Biomech. Model. Mechanobiol.* 11:1001–1013, 2012.
- ¹⁴Cilla, M., E. Peña, and M. A. Martinez. Mathematical modelling of atheroma plaque formation and development in coronary arteries. *J. R. Soc. Interface* 11:20130866, 2014.
- ¹⁵Colton, C. K., S. Friedman, D. E. Wilson, and R. S. Lees. Ultrafiltration of lipoproteins through a synthetic membrane. Implications for the filtration theory of atherogenesis. *J. Clin. Invest.* 51:2472–2481, 1972.
- ¹⁶Cullen, S. A., and R. I. Hill. Aviation pathology and toxicology. In: *Ethics and Mental Health: The Patient, Profession and Community*, edited by D. J. Rainford, and D. P. Gradwell. Boca Raton: CRC Press, 2006, pp. 517–533.
- ¹⁷Darcy, H. Les Fontaines Publiques de la Ville de Dijon. Exposition et Application des Principes à Suivre et des Formules à Employer dans les Questions de Distribution d'Eau. Paris: Victor Dalmont, 1856.
- ¹⁸Duck, F. A. *Physical Properties of Tissues: A Comprehensive Reference Book*. San Diego: Academic Press Inc, p. 336, 1990.
- ¹⁹Eslamian, M. Advances in thermodiffusion and thermophoresis (Soret effect) in liquid mixtures. *FHMT* 2:043001, 2011.
- ²⁰Finegold, J. A., P. Asaria, and D. P. Francis. Mortality from ischaemic heart disease by country, region, and age: statistics from World Health Organisation and United Nations. *Int. J. Cardiol.* 168:934–945, 2013.
- ²¹Gupta, P. K., J. Singh, and K. N. Rai. Numerical simulation for heat transfer in tissues during thermal therapy. *J. Therm. Biol.* 35:295–301, 2010.
- ²²Hao, W., and A. Friedman. The LDL-hdl profile determines the risk of atherosclerosis: a mathematical model. *PLoS ONE* 9:e90497, 2014.
- ²³Hossain, S. S., S. F. A. Hossainy, Y. Bazilevs, V. M. Calo, and T. J. R. Hughes. Mathematical modeling of coupled drug and drug-encapsulated nanoparticle transport in patient-specific coronary artery walls. *Comput. Mech.* 49:213–242, 2012.
- ²⁴Huang, Y., D. Rumschitzki, S. Chien, and S. Weinbaum. A fiber matrix model for the filtration through fenestral pores in a compressible arterial intima. *Am. J. Physiol.* 272:H2023–H2039, 1997.
- ²⁵Huysmans, M., and A. Dassargues. Review of the use of Péclet numbers to determine the relative importance of advection and diffusion in low permeability environments. *Hydrogeol. J.* 13:895–904, 2005.
- ²⁶Jung, H., J. W. Choni, and C. G. Park. Asymmetric flows of non-Newtonian fluids in symmetric stenosed artery. *Korea-Aust. Rheol. J.* 16:101–108, 2004.
- ²⁷Kaazempur-Mofrad, M. R., S. Wada, J. G. Myers, and C. R. Ethier. Mass transport and fluid flow in stenotic arteries: axisymmetric and asymmetric models. *Int. J. Heat Mass Tran.* 48:4510–4517, 2005.
- ²⁸Karner, G., and K. Perktold. Effect of endothelial injury and increased blood pressure on albumin accumulation in the arterial wall: a numerical study. *J. Biomech.* 33:709–715, 2000.
- ²⁹Karner, G., K. Perktold, and H. P. Zehentner. Computational modeling of macromolecule transport in the arterial wall. *Comput. Methods Biomech. Biomed. Eng.* 4:491–504, 2001.
- ³⁰Katz, M. A. New formulation of water and macromolecular flux which corrects for non-ideality: theory and derivation, predictions, and experimental results. *J. Theor. Biol.* 112:369–401, 1985.
- ³¹Kays, W. M., and M. E. Crawford. *Convective Heat and Mass Transfer*. New York: McGraw-Hill, p. 512, 1993.
- ³²Kedem, O., and A. Katchalsky. Thermodynamic analysis of the permeability of biological membranes to non-electrolytes. *Biochim. Biophys. Acta* 27:229–246, 1958.
- ³³Keller, B., F. Clubb Jr., and G. Dubini. A review of atherosclerosis and mathematical transport models. In: *IF-MBE Proceedings, Vol. 36*, edited by S. Vlad, and R. V. Ciupa. Berlin: Springer, 2011, pp. 338–343.
- ³⁴Kenjereš, S., and A. de Loo. Modelling and simulation of low-density lipoprotein transport through multi-layered wall of an anatomically realistic carotid artery bifurcation. *J. R. Soc. Interface* 11:20130941, 2014.
- ³⁵Khakpour, M., and K. Vafai. Effects of gender-related geometrical characteristics of aorta-iliac bifurcation on hemodynamics and macromolecule concentration distribution. *Int. J. Heat Mass Tran.* 51:5542–5551, 2008.
- ³⁶Khakpour, M., and K. Vafai. Critical assessment of arterial transport models. *Int. J. Heat Mass Tran.* 51:807–822, 2008.
- ³⁷Khamdaengyodtai, P., K. Vafai, P. Sakulchangsattajai, and P. Terdtoon. Effects of pressure on arterial failure. *J. Biomech.* 45:2577–2588, 2012.
- ³⁸Kiousis, D. E., T. C. Gasser, and G. A. Holzapfel. A numerical model to study the interaction of vascular stents with human atherosclerotic lesions. *Ann. Biomed. Eng.* 35:1857–1869, 2007.
- ³⁹Kolios, M. C., M. D. Sherar, and J. W. Hunt. Large blood vessel cooling in heated tissues: a numerical study. *Phys. Med. Biol.* 40:477–494, 1995.
- ⁴⁰Liu, X., Y. Fan, and X. Deng. Effect of the endothelial glycocalyx layer on arterial LDL transport under normal and high pressure. *J. Theor. Biol.* 283:71–81, 2011.
- ⁴¹Mahjoob, S., and K. Vafai. Analytical characterization of heat transport through biological media incorporating hyperthermia treatment. *Int. J. Heat Mass Tran.* 52:1608–1618, 2009.
- ⁴²Malvè, M., C. Serrano, E. Peña, R. Fernández-Parra, F. Lostalé, M. A. De Gregorio, and M. A. Martinez. Modelling the air mass transfer in a healthy and a stented rabbit trachea: CT-images, computer simulations and experimental study. *Int. Commun. Heat. Mass* 53:1–8, 2014.
- ⁴³Mandal, D. K., N. K. Manna, and S. Chakrabarti. Influence of different bell-shaped stenoses on the progression of the disease, atherosclerosis. *J. Mech. Sci. Technol.* 25:1933–1947, 2011.
- ⁴⁴Meyer, G., R. Merval, and A. Tedqui. Effects of pressure-induced stretch and convection on low-density lipoprotein and albumin uptake in the rabbit aortic wall. *Circ. Res.* 79:532–540, 1996.
- ⁴⁵Misra, J. C., and G. C. Shit. Blood flow through arteries in a pathological state: a theoretical study. *Int. J. Eng. Sci.* 44:662–671, 2006.
- ⁴⁶Olgac, U., V. Kurtcuoglu, and D. Poulidakos. Computational modeling of coupled blood-wall mass transport of LDL: effects of local wall shear stress. *Am. J. Physiol. Heart Circ. Physiol.* 294:H909–H919, 2008.
- ⁴⁷Platten, J. K. The Soret effect: a review of recent experimental results. *J. Appl. Mech.* 73:5–15, 2006.
- ⁴⁸Prosi, M., P. Zunino, K. Perktold, and A. Quarteroni. Mathematical and numerical models for transfer of low-density lipoproteins through the arterial walls: a new methodology for the model set up with applications to the study of disturbed luminal flow. *J. Biomech.* 38:903–917, 2005.

- ⁴⁹Rahman, M. A., and M. Z. Saghir. Thermomdiffusion or Soret effect: historical review. *Int. J. Heat Mass Tran.* 73:693–705, 2014.
- ⁵⁰Sáez, P., E. Peña, M. A. Martínez, and E. Kuhl. Computational modeling of hypertensive growth in the human carotid artery. *Comput. Mech.* 53:1183–1196, 2014.
- ⁵¹Seeley, B. D., and D. F. Young. Effect of geometry on pressure losses across models of arterial stenosis. *J. Biomech.* 9:447–448, 1976.
- ⁵²Stangeby, D. K., and C. R. Ethier. Computational analysis of coupled blood-wall arterial LDL transport. *J. Biomech. Eng.* 124:1–8, 2002.
- ⁵³Stark, J. R., J. M. Gorman, E. M. Sparrow, J. P. Abraham, and R. E. Kohler. Controlling the rate of penetration of therapeutic drug into the wall of an artery by means of a pressurized balloon. *J. Biomed. Sci. Eng.* 6:527–532, 2013.
- ⁵⁴Steiner, R. Laser-tissue interactions. In: *Laser and IPL Technology in Dermatology and Aesthetic Medicine*, edited by S. Karsai, and C. Raulin. Berlin: Springer Berlin Heidelberg, 2011.
- ⁵⁵Sun, N., R. Torii, N. B. Wood, A. D. Hughes, S. A. Thom, and X. Y. Xu. Computational modeling of LDL and albumin transport in an in vivo CT image-based human right coronary artery. *J. Biomech. Eng.* 131:021003, 2009.
- ⁵⁶Sun, N., N. B. Wood, A. D. Hughes, S. A. M. Thom, and X. Y. Xu. Effects of transmural pressure and wall shear stress on LDL accumulation in the arterial wall: a numerical study using a multilayered model. *Am. J. Physiol. Heart Circ. Physiol.* 292:H3148–H3157, 2007.
- ⁵⁷Tada, S., and J. M. Tarbell. Interstitial flow through the internal elastic lamina affects shear stress on arterial smooth muscle cells. *Am. J. Physiol. Heart Circ. Physiol.* 278:H1589–H1597, 2000.
- ⁵⁸Tarbell, J. M. Mass transport in arteries and the localization of atherosclerosis. *Annu. Rev. Biomed. Eng.* 5:79–118, 2003.
- ⁵⁹Taylor, F., M. D. Huffman, A. F. Macedo, T. H. Moore, M. Burke, G. Davey Smith, K. Ward, and S. Ebrahim. Statins for the primary prevention of cardiovascular disease. *Cochrane Database Syst. Rev.* 1:CD004816, 2013.
- ⁶⁰Vafai, K., and C. L. Tien. Boundary and inertia effects on flow and heat transfer in porous media. *Int. J. Heat Mass Tran.* 24:195–203, 1981.
- ⁶¹Wada, S., and T. Karino. Computational study on LDL transfer from flowing blood to arterial walls. In: *Clinical Application of Computational Mechanics to the Cardiovascular System*, edited by T. Yamaguchi. Tokyo: Springer Japan, 2000, pp. 157–173.
- ⁶²Wakeham, W. A., A. Nagashima, and J. V. Sengers. *Experimental Thermodynamics, Vol. III, Measurement of the Transport Properties of Fluids, Vol. III.* Oxford: Blackwell Scientific Publications, 1991.
- ⁶³Xie, X., J. Tan, D. Wei, D. Lei, T. Yin, J. Huang, X. Zhang, J. Qiu, C. Tang, and G. Wang. In vitro and in vivo investigations on the effects of low-density lipoprotein concentration polarization and haemodynamics on atherosclerotic localization in rabbit and zebrafish. *J. R. Soc. Interface* 10:20121053, 2013.
- ⁶⁴Yang, F., G. Holzapfel, C. Schulze-Bauer, R. Stollberger, D. Thedens, L. Bolinger, A. Stolpen, and M. Sonka. Segmentation of wall and plaque in in vitro vascular MR images. *Int. J. Cardiovasc. Imaging* 19:419–428, 2003.
- ⁶⁵Yang, N., and K. Vafai. Modeling of low-density lipoprotein (LDL) transport in the artery—effects of hypertension. *Int. J. Heat Mass Tran.* 49:850–867, 2006.
- ⁶⁶Young, D. F., and F. Y. Tsai. Flow characteristics in models of arterial stenoses: I. *Steady flow.* *J. Biomech.* 6:395–410, 1973.